

Journal of Materials Chemistry A

Accepted Manuscript

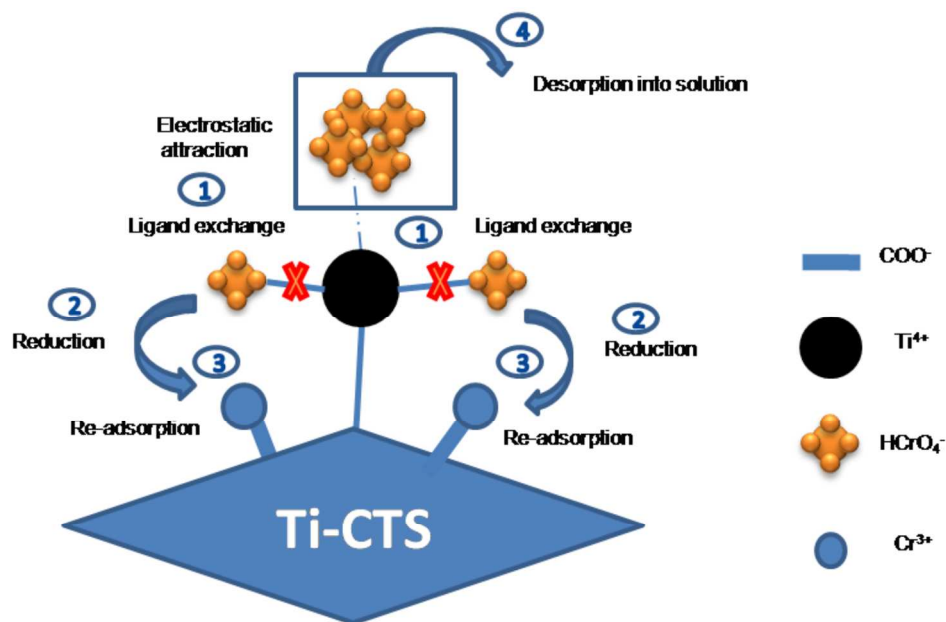


This is an *Accepted Manuscript*, which has been through the Royal Society of Chemistry peer review process and has been accepted for publication.

Accepted Manuscripts are published online shortly after acceptance, before technical editing, formatting and proof reading. Using this free service, authors can make their results available to the community, in citable form, before we publish the edited article. We will replace this *Accepted Manuscript* with the edited and formatted *Advance Article* as soon as it is available.

You can find more information about *Accepted Manuscripts* in the [Information for Authors](#).

Please note that technical editing may introduce minor changes to the text and/or graphics, which may alter content. The journal's standard [Terms & Conditions](#) and the [Ethical guidelines](#) still apply. In no event shall the Royal Society of Chemistry be held responsible for any errors or omissions in this *Accepted Manuscript* or any consequences arising from the use of any information it contains.



610x378mm (96 x 96 DPI)

Synthesis of titanium cross-linked chitosan composite for efficient adsorption and detoxification of hexavalent chromium from water

Lingfan Zhang^{a,b}, Wei Xia^a, Xin Liu^{a*} and Wenqing Zhang^{a**}

^a School of Chemistry and Molecular Engineering, East China University of Science and

5 Technology, Shanghai 200237, PR China

^b Research Center of Analysis and Test, East China University of Science and Technology,

Shanghai 200237, PR China

* Corresponding author: Xin Liu Tel.: +86-21-64253225 Fax: +86-21-64252947

E-mail address: liuxin@ecust.edu.cn

10 ** Corresponding author: Prof. Wenqing Zhang Tel.: +86-21-64253401 Fax: +86-21-64252947

E-mail address: zhwqing@ecust.edu.cn

15

20

Abstract

For simultaneous adsorption and detoxification of hexavalent chromium from
25 water, a new titanium-chitosan (Ti-CTS) composite was synthesized through the
metal-binding reaction between titanium ions and chitosan biopolymer then
cross-linked with glutaraldehyde. The resultant composite was characterized by FT-IR,
XRD, Elemental Mapping, SEM and XPS. The adsorption properties toward Cr(VI)
were systematically investigated as a function of pH, dosage, initial concentration,
30 contact time, temperature and co-existing ions. Experimental data were well described
by Langmuir isotherm and pseudo-second order model, with the maximum adsorption
capacity 171 mg g^{-1} . More attractively, the Cr(VI) could be effectively absorbed and
reduced to less toxic Cr(III) by Ti-CTS composite. The experimental results, FT-IR
and XPS indicated that the possible removal mechanism of Cr(VI) onto Ti-CTS
35 composite was summarized into three steps: (i) Cr(VI) adsorption by electrostatic
attraction (Ti^{4+} and HCrO_4^-) and ligand exchange (Cl^- and HCrO_4^-); (ii) Cr(VI) partly
reduced to Cr(III); (iii) re-adsorption Cr(III) onto Ti-CTS composite.

40

45 **Keywords:** titanium-chitosan composite; hexavalent chromium; adsorption;
detoxification.

50

55

60

65

1. Introduction

Chromium is a common pollutant in the environment which discharges from various industry processes such as leather tanning, electroplating and water cooling.¹

70 Chromium exists two species in natural waters: Cr(III) and Cr(VI). The former is essential for the proper functioning of living organisms and is less toxic than later species.² However, Cr(VI) is a highly soluble reactive and mobile species in aquatic systems, thus exerting carcinogenicity and toxicity to biological systems due to its strong oxidizing properties.³ Due to its hazard, Cr(VI) must be removed from

75 wastewater prior discharged into the environment.⁴ Traditionally, two types of treatment technologies are always used to remove Cr(VI) from wastewater: the first type reduces Cr(VI) to Cr(III) followed by chemical precipitation, while the second type removes Cr(VI) directly.⁵ Currently, simultaneous adsorption and detoxification of Cr(VI) is considered as the most economical and effective method.⁶ Many of

80 adsorbents have been reported for detoxification of Cr(VI) contaminated waters, such as polypyrrole/cellulose fiber composite,⁷⁻⁸ tannic acid immobilized powdered activated carbon with humic acid⁹ and based zero-valent iron nanoparticles.^{2, 10}

However, the abovementioned adsorbents either had weak mechanical strength, low adsorption capacity or easily susceptible to oxidation and agglomeration. These

85 drawbacks have limited the applications for Cr(VI) removal from wastewater. It is necessary to develop new adsorbents with high adsorption capacity and stability for Cr(VI) removal, especially simultaneous Cr(VI) adsorption and reduction.

Chitosan (CTS) is one of the important natural polymers composed by layers of

crustaceans and cell walls of many fungi. And it is a reproducible and environmental friendly material and has been found to be capable of chemically or physically adsorbing various heavy metal ions.¹¹ Recently, metal-based chitosan have been reported to be highly efficient in the removal of Cr(VI) in wastewater. For example, chitosan/Fe⁰ nanoparticles were prepared for adsorption of hexavalent chromium from wastewater by some researchers.^{4, 11-13} Zimmermann et al reported Fe-crosslinked chitosan complex could effectively remove Cr(VI) from aqueous solution.¹⁴ And the chitosan-Fe(III) complex was also applied to study the mechanism of detoxification of Cr(VI) by Shen.¹⁵ Besides, titania-based adsorbents were also reported for adsorption contaminant from wastewaters. It was reported that titanium hydroxide-derived adsorbent¹⁶ and crystalline titanium dioxide¹⁷ were prepared for adsorption fluoride ions from aqueous solution. TiO₂-impregnated chitosan beads as a novel bio-based adsorbent have been prepared for arsenic removal by Miller.¹⁸ And the metal-binding of chitosan was also used to incorporate titanium metal and applied as an adsorbent for fluoride adsorption.¹⁹ To our best of knowledge, however, no report has been published about titanium(VI) binding with chitosan for Cr(VI) adsorption and reduction.

The aim of this study was to synthesize a titanium-chitosan composite for adsorption and reduction of Cr(VI) from water. The main objectives were: (1) to synthesize and characterize the titanium-chitosan composite, (2) to evaluate the influence of different factors on the Cr(VI) adsorption by Ti-CTS composite, (3) to study the adsorption isotherms and kinetics of these reactions, (4) to test the role of

chitosan in Cr(VI) reduction by Ti-CTS composite, as well as Chromium species of final products, and (5) to explore the reaction mechanism of this composite for Cr(VI) removal.

2. Materials and methods

115 2.1. Materials

Chitosan (food grade, 91% deacetylation degree, with average molecular weight of 4.0×10^5 g mol⁻¹) was supplied by Shanghai Weikang Biological Co. (China). Tetrabutyl titanate (analytical grade), acetate acid, sodium hydroxide were purchased from Sinopharm Chemical Reagent Co., Ltd (China). Glutaraldehyde was purchased
120 from Merck (China). The standard solution (Cr(VI), 1000 mg L⁻¹) was fresh prepared by dissolving appropriate potassium dichromate (K₂Cr₂O₇) in distilled water. All other chemicals used were analytical reagent grade, and all solutions were prepared with distilled water without further purification.

2.2. Preparation of Ti-CTS composite

125 The Ti-CTS composite was synthesized according to the method in previous reported literature with some modification.^{19, 20} In detail, 3.22 g chitosan powder was added into 100 mL 2% (v/v) acetic acid aqueous solution and mixed until the chitosan dissolved completely. Titanium solution was prepared by adding 5 mL concentrated HCl to 3.42 g of tetrabutyl titanate. This titanium solution was slowly added into
130 chitosan solution under stirring at 150 rpm for 2 h. Subsequently, the Ti-CTS composite was precipitated by dropwise adding 2.0 M sodium hydroxide solution with continuous stirring to obtain the composite. Then, 5 mL 5% of glutaraldehyde

aqueous solution was added and stirred vigorously with cross-linked reaction for 2 h more. After reaction, the composite was separated from solution and washed with distilled water to neutral pH followed by drying at 40°C for 2 days. The dried composite was used for chromium adsorption studies.

2.3. Characterization and measurement

The FTIR spectra of CTS, Ti-CTS and Ti-CTS loaded Cr(VI) were recorded by using Nicolet 6700 FTIR spectrometer (Thermo Electron Corporation) in the range 4000 ~ 400 cm^{-1} with a resolution of 4 cm^{-1} in transmittance mode. X-ray diffraction (XRD) pattern of Ti-CTS composite before and after adsorption of Cr(VI) were performed by rotating anode X-ray powder diffractometer (D/MAX 2550 VB/PC, Rigaku corporation) with Cu $K\alpha$ characteristic radiation. All samples were scanned from 5° to 80° (2 θ) at a scanning rate of 3° (2 θ) per minute. Elemental mapping images of Ti-CTS composite before and after Cr(VI) adsorption were obtained by Transmission Electron Microscopy–Energy Dispersive X-ray Spectroscopy (TEM-EDXS, Genesis XM2 system, USA EDAX corporation). Scanning electronic microscopy (SEM) images were obtained on a JSM-6360LV scanning electron microscopy. XPS spectra were obtained using Thermo Scientific ESCALAB 250Xi X-ray photoelectron spectrometer (XPS) system (Al $K\alpha$ X-ray source was used). The XPS spectra were fitted assuming Gaussian-Lorentzian distribution for each peak in order to determine the binding energy of the element core levels, and all binding energies were referenced to the neutral carbon peak at 285.0 eV. All of the XPS spectra were normalized.

155 The concentration of total Cr in solution was determined by inductively coupled plasma optical emission spectrometer (ICP-OES 710 series, Agilent, USA). The residual Cr(VI) in solution was measured by the diphenylcarbohydrazide method. The absorbance of purple Cr(VI)-diphenylcarbohydrazide product was formed after 10 min and measured by using a 722N UV-Vis spectrophotometer at wavelength of 540
160 nm (Shanghai Precision & Scientific Instrument Co., Ltd). The concentration of Cr(III) was calculated based on the difference between the total Cr and Cr(VI) concentrations.

2.4. Adsorption of Chromium on Ti-CTS composite

Batch adsorption experiments were carried out to evaluate the adsorption
165 capacities of Ti-CTS composite. A series of 250 mL reagent bottles containing 100 mL Cr(VI) solutions and 20 mg of Ti-CTS composite were shaken at 150 rpm for a certain time. The sample pH was adjusted to the desired value with 0.1 M HCl or 0.1 M NaOH. The concentration of chromium in the initial or equilibrium solutions were determined by ICP-OES or UV. The adsorption capacities were defined as the
170 following equation:

$$q_e = \frac{C_o - C_e}{W} V \quad (1)$$

Where q_e is the amount of adsorbent in solid phase (mg g^{-1}); C_o and C_e is the initial and equilibrium concentration of chromium in the liquid phase (mg L^{-1}), respectively; V is the volume of the solution (L) and W is the mass of Ti-CTS composite (g).

175 3. Results and discussion

3.1. Characterization of Ti-CTS composite

Please insert Fig. 1, here

Fig. 1A showed the FT-IR spectra of CTS, Ti-CTS composite and Cr(VI) loaded Ti-CTS composite (Ti-CTS-Cr). The main characteristic peaks of CTS (a) were at 3443 cm^{-1} ($-\text{OH}$ and $-\text{NH}_2$ stretching vibrations), 2922 cm^{-1} ($-\text{CH}$ stretching vibration), 1657 cm^{-1} ($-\text{NH}_2$ bending vibration), 1382 cm^{-1} ($-\text{CH}$ symmetric bending vibration), 1081 cm^{-1} ($\text{C}-\text{O}$ stretching at C3) and 1034 cm^{-1} ($\text{C}-\text{O}$ stretching at C6).²¹ For FT-IR spectrum of Ti-CTS (b), the $-\text{NH}_2$ bending at 1636 cm^{-1} had a shift of 21 cm^{-1} when compared with CTS, which confirmed that Ti^{4+} ions have been interacted with $-\text{NH}_2$ group present in CTS. Besides, The two bands at 1081 cm^{-1} and 1034 cm^{-1} corresponding to $\text{C}-\text{OH}$ stretching at C3 and C6 were merged into one band and transferred to 1086 cm^{-1} (with a shift 5 cm^{-1}). This might be due to the interaction of $-\text{OH}$ group in CTS with the Ti^{4+} .²² Furthermore, the band at around 3420 cm^{-1} attributed to $-\text{NH}_2$ and $-\text{OH}$ stretching vibration in Ti-CTS has been shifted 23 cm^{-1} in Ti-CTS which indicated Ti^{4+} ions have been bended onto amino and hydroxyl groups of CTS. Additionally, the broad bands at 900 ~ 400 cm^{-1} revealed for $\text{Ti}-\text{O}$ vibration and Ti Lewis sites with the NH_2 groups from chitosan chain.²³⁻²⁴ After adsorption of Cr(VI), the FT-IR spectrum of Ti-CTS-Cr (c) found two new peaks at 901 cm^{-1} and 804 cm^{-1} which was due to $\text{Cr}-\text{O}$ stretching and asymmetric vibration, respectively.^{10,25} More importantly, strong peak appeared at 1632 cm^{-1} was attributed to stretch vibration of $\text{C}=\text{O}$, and the decrease in $\text{C}-\text{O}$ stretch band at 1034 cm^{-1} indicated that the carboxylated had formed at the C6 position of CTS.²⁶ Besides, the band gaps (E_g) were also calculated via FT-IR spectra according to the

Tauc/Davis-Mott Model²⁷. The values of E_g for Ti-CTS and Ti-CTS-Cr composite were 0.586 eV and 0.577 eV ($n=2$), respectively. The E_g had a slight decrease after adsorption of Cr(VI), which suggested that the presence of Cr(VI) would modify the electronic states and optical transitions of the composite and resulted in allowed transitions.

The XRD patterns of CTS, Ti-CTS and Ti-CTS-Cr composite in the range of $2\theta = 3 \sim 80^\circ$ were shown in Fig. 1B. CTS (a) showed characteristic peaks at $2\theta = 10.5^\circ$, 19.7° , 35.5° and 40.3° , which were attributed to be (001), (100), (101) and (002) plan, respectively.²⁸ XRD spectrum of Ti-CTS composite was depicted in Fig. 1B-b. Only one extraordinary broad peak was observed and the position at $2\theta = 19.7^\circ$ was shifted to 25.6° . This was due to the conjugation of Ti^{4+} and chitosan, which decreased the crystalline nature to some extent. Therefore, the results confirmed the incorporation of Ti^{4+} ions into CTS. Fig. 1B-c demonstrated the XRD spectrum of Ti-CTS-Cr composite which showed that the peak transferred to 26.2° after adsorption of Cr(VI).

Elemental mapping image (EMI) was carried out to confirm the presence and distribution of elements in the composite. The EMI spectra of the Ti-CTS composite before and after Cr(VI) adsorption were showed in Fig. 1C. In order to improve the element resolution, the C, O and N elements were omitted in the images. From the EMI images, the presence of Cl and Ti were clearly observed in the Ti-CTS composite and the elemental distribution was uniform. This clearly confirmed the incorporation of Ti^{4+} ions into chitosan matrix. After adsorption, the element of Cr was presented in the EMI images, indicating Cr(VI) adsorption occurred onto the composite. Moreover,

The Cr and Ti elements on the Ti-CTS-Cr composite were well-distributed which further confirmed the Cr(VI) ions were successfully absorbed through the active sites on the surface of Ti-CTS composite. Besides, the element of Cl was disappeared after adsorption of Cr(VI), suggested that there had a ligand exchange reaction between the coordinated chlorate and Cr(VI) ions. Moreover, the SEM images of CTS, Ti-CTS and Ti-CTS-Cr were shown in Fig. 1D, 1E and 1F. The surface of CTS (D) and Ti-CTS composite (E) was non-porous and flat. However, the rough surface was formed for the Ti-CTS-Cr (F). This was due to the accumulation of Cr(VI) by adsorption mechanism.

The XPS wide scan spectra of Ti-CTS composite before and after Cr(VI) adsorption were also analyzed and shown in Fig. 2A and 2B. From the figures, the major peaks such C 1s, O 1s, N 1s, Ti 2p and Cl 2p₃ were present. A new peak assigning to Cr 2p was clearly observed and the peak of Cl 2p₃ was simultaneously disappeared after Cr(VI) adsorption, which also confirmed the adsorption of Cr onto Ti-CTS composite through ligand exchange. These results were consistent with the EMI analysis.

Please insert Fig. 2, here

3.2. Effect of pH

The removal of Cr(VI) from aqueous solution was highly dependent on the pH of solution because the pH affected not only the surface charges of the adsorbent but also the Cr species during the reaction. In this experiment, the initial pH of solutions (30 mg L⁻¹ Cr(VI)) were adjusted to the range of 2 ~ 9 using HCl or NaOH and its effects

on Cr(VI) removal was explored. The results were shown in Fig. 3a. From the Fig. 3a, the removal efficiency of Cr(VI) by Ti-CTS composite was notably higher in an acidic medium than in an alkaline medium. The residual Cr concentration increased as the pH increased from 5.0 to 9.0. However, the Cr(III) species accounted for a certain proportion of the residual total Cr concentration at $2 < \text{pH} < 4.0$, which was due to the fact that the protons participated in the reduction reaction in low pH solution as equation (2).²⁹ Therefore, the optimal pH values for Cr(VI) removal was 5.0 corresponding to a Cr(VI) adsorption capacity of 123 mg g^{-1} .



At the optimum of pH 5, the chromium species in solution was mainly HCrO_4^- (around 97 %).¹⁴ And the Ti^{4+} of Ti-CTS composite could be also protonated and increased positively charge on the surface, which resulted in a stronger electrostatic attraction for chromium anions (HCrO_4^-). Therefore, chromium adsorption at pH 5.0 onto Ti-CTS composite occurred via electrostatic attraction between Ti^{4+} and HCrO_4^- ions. Combined with the element of Cl disappeared by XPS spectra, Ti-CTS composite for the adsorption of the Cr(VI) could be considered as ligand-exchange reaction between the coordinated Cl^- and HCrO_4^- and electrostatic attraction by Ti^{4+} as adsorption sites for HCrO_4^- ions. Above pH 5, the residual Cr(VI) concentration was increased as pH increased. The reasons were given as follows: (1) the pH_{zpc} of Ti-CTS composite was 8.1 measured by pH drafted method³⁰ and the net surface charge became less positive with increasing the pH, which resulted in repulsive forces between Ti-CTS composite and Cr(VI); (2) the higher concentration of OH^- ions

265 presented in the high pH solution, which competed with HCrO_4^- ions for the adsorption sites; (3) the chromium species were CrO_4^{2-} and $\text{Cr}_2\text{O}_7^{2-}$ in alkaline medium, which also decreased the Ti-CTS composite capacity for Cr(VI) adsorption. Furthermore, it was very interesting to note that at $\text{pH} > 4$, Cr(III) concentration of the reaction solutions were only negligible, indicating that once Cr(VI) was converted to
270 Cr(III), the Cr(III) was effectively adsorbed onto the composite. Thus, the subsequently experiments were conducted at optimum condition of pH 5 and the chromium species was only discussed Cr(VI) in solutions.

In addition, in order to check the stability and chemical resistance in acidic media of Ti-CTS composite, the Ti^{4+} ions released in Cr(VI) adsorption solution was
275 analyzed by ICP-OES at pH 2 ~ 8 (Fig. 3a-Ti). The results showed that the concentration of Ti^{4+} ions leaching in solution was only found 0.10 ~ 0.46 mg L^{-1} when the pH was from 2.0 to 4.0, but very low concentration was found at above pH 5, which confirmed that Ti-CTS composite became more resistant to lower pH compared to their parent chitosan which dissolved completely at pH 5.³¹

280

Please insert Fig. 3, here

3.3. Effect of adsorbent dose

The adsorbent dose of Ti-CTS composite was varied (10-100 mg/100 mL) while keeping fixed the concentration of Cr(VI) in solution. Fig. 3b illustrated the effect of adsorbent dose on adsorption of Cr(VI). The higher adsorption capacities were
285 observed for 10 mg and 20 mg of composite, which gradually decreased with increasing weight of Ti-CTS composite. The high adsorption observed for 10 mg and

20 mg composite was attributed to easy accessibility of free active sites on surface of adsorbent. On increasing weight of Ti-CTS composite, the number of active sites increased but ratios of Cr(VI) to active sites decreased resulting in gradual decrease of adsorption. Considering to the ratios of Cr(VI) and adsorption capacity, the optimum dose for Cr(VI) was chosen 20 mg/100 mL in the following adsorption study.

3.4. Effect of initial concentration of Cr(VI) and adsorption isotherm

The effect of initial Cr(VI) concentration on the adsorption capacity was carried out in the range of 10 ~ 60 mg L⁻¹ with fixed contact time (10 h) and pH 5.0. The results in Fig. 3c showed the uptake of Cr(VI) on Ti-CTS composite gradually increased as the initial concentration increased until the saturation point was attained at 50 mg L⁻¹, thereafter there reached the plateau. This was due to the fact that the available sites for adsorption remained constant for a fixed amount of Ti-CTS composite.

For interpretation of the adsorption data, the equilibrium adsorption of this process was described by applying the Langmuir, Freundlich and Tempkin isotherm models.

The linear form of Langmuir, Freundlich and Tempkin equation can be represented as follows, respectively:

$$\frac{C_e}{q_e} = \left(\frac{1}{k_L q_{\max}} \right) + \left(\frac{C_e}{q_{\max}} \right) \quad (3)$$

$$\ln q_e = \ln k_F + \frac{1}{n} (\ln C_e) \quad (4)$$

$$q_e = \frac{RT}{b} (\ln A) + \frac{RT}{b} (\ln C_e) \quad (5)$$

Where C_e is the equilibrium concentration of adsorbate in solution (mg L^{-1}); q_e and q_{max} (mg g^{-1}) are the amount adsorbed at equilibrium and the maximum adsorption capacity for monolayer formation on adsorbent, respectively. k_L (L mg^{-1}) is the langmuir constant related to the maximum adsorption capacity and the energy of adsorption. k_F is Freundlich constant and n is the heterogeneity factor. The constant B (RT/b) is related to the heat of adsorption.

The value of theoretical parameters and constants could be calculated from the intercept and slope of the linear equation, respectively. The results were summarized in Table 1. For the three studied isotherm models (Fig. 3c), the Langmuir isotherm ($R^2 = 0.993$) correlated better than Freundlich and Tempkin with the equilibrium data for the adsorption of Cr(VI) on Ti-CTS composite, suggesting a monolayer adsorption. The maximum adsorption value (171 mg g^{-1}) was in good accordance with experimentally obtained value (167 mg g^{-1}). The proposed Ti-CTS composite was compared with other adsorbents recently reported literature (listed in Table 2). It could be seen that the maximum adsorption capacity of Ti-CTS was higher than other reported adsorbents.^{28, 32-39} Besides, the value of n in Freundlich isotherm was in range of $1 \sim 10$ represented a good adsorption.⁴⁰ In this work, the exponent of n was 2.54 ($1 < n < 10$), indicating that the adsorption system was favorable.

Please insert Table 1, here.

Please insert Table 2, here.

3.5. Effect of contact time and adsorption kinetics

Batch experiments about the adsorption kinetics for the removal of Cr(VI) on

330 Ti-CTS composite were executed using the initial concentration of 30 and 50 mg L⁻¹ at pH 5. As shown in Fig. 3d, the adsorption capacity of Cr(VI) onto Ti-CTS composite increased with an increase in contact time. More than 80% of the Cr(VI) was absorbed by Ti-CTS composite at the first 30 min. The rapid adsorption in the beginning could be attributed to the greater concentration gradient and more available
 335 sites for adsorption. Besides, the initial Cr(VI) concentration had obviously effect on the adsorption process to reach the equilibrium. The time needed to reach the equilibrium for the initial Cr(VI) concentration of 30 mg L⁻¹ was 4 h, while it took about 7 h for initial Cr(VI) concentration of 50 mg L⁻¹.

To order to investigate the rate-controlling mechanism of adsorption process, the
 340 kinetic data were correlated to linear forms of the pseudo-first order rate model and the second-order rate model.

$$\text{Pseudo-first order equation: } \log(q_e - q_t) = \log q_e - \frac{k_1}{2.303} t \quad (6)$$

$$\text{Pseudo-second order equation: } \frac{t}{q_t} = \frac{1}{k_2 q_e^2} + \frac{t}{q_e} \quad (7)$$

Where q_t and q_e are the amounts of metal ion adsorbed at time t (min) and
 345 equilibrium. k_1 (min⁻¹) and k_2 (g (mg min)⁻¹) are the pseudo-first-order and pseudo-second-order rate constant of adsorption, respectively. The value of the rate constants were also calculated from the intercept and slop of the curves. The initial adsorption rate (h , mg g⁻¹ min⁻¹) could be calculated from $h = k_2 q_e^2$. After simulating the kinetics data, unfortunately, the pseudo-first order kinetic model was insufficient
 350 to describe the adsorption process of Cr(VI) with low correlation coefficients ($R^2 < 0.9$, the result was not given here). However, the pseudo-second order rate model

showed good linearity at two different initial Cr(VI) concentrations and the calculated correlation coefficients (R^2) were all higher than 0.999 (see Table 1). The theoretical q_e values were very close to the experimental values and the adsorption rate h were found to decrease with an increase of the initial Cr(VI) concentration, suggesting a more rapid adsorption of Cr(VI) onto Ti-CTS composite at a lower initial concentration. These results indicated that the adsorption of Cr(VI) onto Ti-CTS composite followed the pseudo-second order rate model and the overall process appeared to be controlled by chemisorption and no involvement of a mass transfer in solution.⁴¹

3.6. Thermodynamic study

To study the thermodynamics of adsorption of Cr(VI) on Ti-CTS composite, the thermodynamic parameters, free energy change (ΔG^0), enthalpy change (ΔH^0) and entropy change (ΔS^0) were estimated by using the following equations:

$$\ln(k_d) = \frac{\Delta S^0}{R} - \frac{\Delta H^0}{RT} \quad (8)$$

$$\Delta G^0 = \Delta H^0 - T\Delta S^0 \quad (9)$$

Where k_d is the adsorption distribution coefficient at different temperatures and the value was calculated by the ratio of q_e to C_e ($k_d = q_e C_e^{-1}$). R is the universal gas constant ($8.314 \text{ J (mol K)}^{-1}$). ΔH^0 and ΔS^0 were calculated by the slope and intercept of the linear plot of $\ln(k_d)$ vs. $1/T$, respectively. The ΔG^0 were obtained from the equation (9) at different temperatures. The values of the thermodynamic parameters were listed in Table 3. The negative ΔG^0 at all temperatures demonstrated that Cr(VI) adsorption over Ti-CTS composite was spontaneous and feasible. Besides, it was

found that the absolute values of ΔG^0 increased with adsorption temperature, suggesting that high temperature was in favor of the increase of adsorption impetus and promoted Cr(VI) adsorption. Moreover, the positive value of ΔH^0 indicated that the adsorption process was endothermic in nature, and the observed positive value of ΔS^0 showed the increased randomness state at the solid-solution interface during the fixation of adsorbate on the active sites of the adsorbent.

Please insert Table 3 here.

3.7. Interference of co-ions

By keeping 20 mg dosage of Ti-CTS composite and 30 mg L⁻¹ (100 mL) as initial Cr(VI) concentration at pH 5, the adsorption capacity was evaluated by different concentrations of co-existing cations (Fe³⁺, Cu²⁺, Zn²⁺, K⁺, Na⁺, Ca²⁺, Mg²⁺) and anions (Cl⁻, NO₃⁻ and SO₄²⁻). The results were depicted in Fig. 3e. From the figure, on one hand, the presence 50 mg L⁻¹ of Fe³⁺, Cu²⁺, Zn²⁺ and 100 mg L⁻¹ of K⁺, Na⁺, Ca²⁺, Mg²⁺ showed no significant interference on the adsorption of Cr(VI). On the other hand, the uptake of Cr(VI) was decreased as increasing the concentration of co-anions. At 200 mg L⁻¹ concentration of Cl⁻ and NO₃⁻, there was a slight effect on the adsorption capacity, while decreased by 18 % and 15 % respectively as increasing the concentration to 500 mg L⁻¹. In addition, SO₄²⁻ had more effect on the adsorption capacities, the percent of adsorption capacities were decreased to 43 % and 33 % when the concentrations were 200 and 500 mg L⁻¹, respectively. This indicated that certain competition between Cl⁻, NO₃⁻ and SO₄²⁻ with Cr(VI) anions for the interaction with active sites on the surface of Ti-CTS composite.

3.8. Chromium species on composite after adsorption

The high resolution of XPS patterns of Ti-CTS composite with and without Cr(VI) adsorption were conducted and shown in Fig. 2C and 2D. Interestingly, the Cr(VI) adsorbed onto the Ti-CTS composite was partially reduced to relatively nontoxic Cr(III) based on the surface chemical compositions of the Ti-CTS composite during removal process. From Fig. 2C, Cr 2p_{1/2} and Cr 2p_{3/2} line peaks were located at around 587.2 eV and 577.7 eV. The broad peak of Cr 2p_{3/2} was deconvoluted into two peaks at binding energies of 577.2 eV and 578.1 eV, which were the characteristic peaks of Cr(III) and Cr(VI), respectively¹. These results suggested that both Cr(VI) and Cr(III) coexisted on the surface of the Cr(VI) adsorbed Ti-CTS composite. To further verify the existence of Cr(III) on the composite, the high resolution XPS spectrum of the Cr 2p region after desorption process were also measured (shown in Fig. 2D). From the Fig. 2D, only one peak was observed with binding energies of 577.2 eV at Cr 2p_{3/2} which belonged to the Cr(III), indicating that partly Cr(VI) adsorbed on the Ti-CTS composite has been reduced to Cr(III).

In order to qualified the Cr(III) and Cr(VI) on the Ti-CTS-Cr composite. After adsorption, the composite was treated with two methods: (a) desorption and digestion: 100 mL of 0.5 mol L⁻¹ NaOH was used to remove chromium for 12 h under stirring at 150 rpm, and then the composite was re-collected and digested with mixed acid (HF/HCl/HClO₄ =1.0 mL/1.0 mL/0.5 mL); (b) direct digestion: the Ti-CTS-Cr composite was digested with the same abovementioned mixed acid. After treatment, the obtained solutions were analyzed for Cr(VI) and Cr(III) concentrations and the

percent of Cr(VI) and Cr(III) were calculated. The results were listed in Table 4. From Table 4, the percent of Cr(VI) in NaOH solution accounted for 99.3 % while the Cr(III) was 0.7 %, suggested that this part of chromium was only absorbed on the Ti-CTS. On the other hand, the content of Cr(III) was 98.7 % in mixed acid digestion solution, which belonged to the reduction of chromium by Ti-CTS composite. The same contents of Cr(VI) and Cr(III) were also obtained with the direct digestion method. Overall, 39.9 % of Cr on the composite was reduced to Cr(III) and the percent of 60.1 % might be only absorbed on the surface of Ti-CTS composite through electrostatic attraction between Ti^{4+} and $HCrO_4^-$.

Please insert Table 4, here.

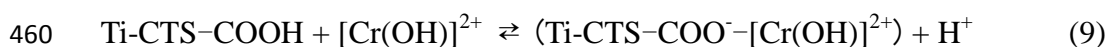
3.9. Regeneration of Ti-CTS composite

In order to investigate the reusability of the Ti-CTS composite, cyclic adsorption-regeneration tests were carried out for Cr(VI) adsorption. As shown in Fig. 3a, the adsorbed capacity was less 10 mg g^{-1} at high pH, indicating that the adsorbed Cr(VI) could be desorbed using alkaline solution. In this study, five concentrations of NaOH solutions including 0.005, 0.01, 0.05, 0.10 and 0.20 mol L^{-1} were used to study the regeneration of Ti-CTS composite. It was found that the desorption ratio was increased until 0.05 mol L^{-1} NaOH was used and thereafter there kept a constant value. Therefore, 0.05 mol L^{-1} NaOH solution was selected for Ti-CTS composite regeneration. Fig. 3-f showed the adsorption abilities of Ti-CTS composite for Cr(VI) during six adsorption-regeneration cycles. At the first cycle, the adsorption capacity had an obvious decrease compared with the original composite. This was because

440 some of active sites were occupied by Cr(III)-complex. Then, in the next five cycles, the adsorption capacities for Cr(VI) only had slight decrease and after six cycles the adsorption capacity still kept 64.9%. This results suggested that the synthesized Ti-CTS composite could be used repeatedly for the treatment of Cr(VI) in wastewater.

3.10. Mechanism of Cr(VI) removal

445 From the results of pH study, the functional groups on the surface of Ti-CTS composite could be protonated and positively charged to form Ti^{4+} in an acidic medium. The protonated surface had a stronger electrostatic attraction for chromium anions ($HCrO_4^-$). On the other hand, the ligand of Cl on the surface Ti-CTS composite would be also exchanged with $HCrO_4^-$ and formed Ti- $HCrO_4$ complex, which was
 450 confirmed by the disappeared of Cl on XPS and EMI analysis. Thus, chemical adsorption occurred because of electrostatic attraction and ligand exchange between the hexavalent chromium aions and the surface active sites, which resulted in complex formation. After adsorption, the ligand exchange of Cr(VI) on the surface of Ti-CTS composite was directly reduced to Cr(III) by the adjacent electron-donor of C-6
 455 alcoholic groups which were oxidized to a carbonyl groups after reaction. Then, these carbonyl groups as dominant functional groups would re-absorb immediately the reduced Cr(III) by ion exchange. The following mechanism has been proposed for the Cr(III) adsorption on the surface of Ti-CTS composite ⁴²:



Therefore, the proposed possible mechanism of adsorption coupled reduction for

Cr(VI) removal by the Ti-CTS composite was presented in scheme 1. The anionic Cr(VI) (HCrO_4^-) were firstly adsorbed onto the Ti-CTS composite by chelation of the Ti^{4+} center in the Ti-CTS complex and by the electrostatic attraction of a protonated sites. Next, the adsorbed Cr(VI) atoms were partially reduced by the adjacent primary alcoholic functions on C-6 which simultaneously were oxidized to carbonyl groups. After that, the coordination bond between the reduced Cr(III) and the Ti^{4+} center in the Ti-CTS composite could be broken, and the free Cr(III) were re-absorbed by Cr-bonding to the Ti-CTS complex. Finally, the only adsorbed Cr(VI) on the composite were desorbed by NaOH into solution. Thus, the Ti-CTS composite could absorb the Cr(VI) and reduced it into less toxic Cr(III) through a rapid and efficient process.

Please insert scheme 1, here.

4. Conclusion

The present study showed that Ti-CTS composite was quite effective for adsorption and detoxification of Cr(VI) in water. The process condition was optimized by the adsorption capacity and leakage concentration of Ti^{4+} . The adsorption data were well described by Langmuir isotherm and kinetics followed the pseudo-second order model, with the maximum adsorption capacity of 171 mg g^{-1} for Cr(VI). The possible removal mechanism for Cr(VI) detoxification was confirmed by the research findings, which consisted of adsorption, reduction and re-adsorption. It is expect that the Ti-CTS composite can be as a promising adsorbent for the treatment of Cr(VI)-contaminated water.

Acknowledgements

485 We are grateful for the financial support by the National Natural Science
Foundation of China (Grant: 21407050).

References

- 1 Ma, H.L., Zhang, Y., Hu, Q.H., Yan, D., Yu, Z.Z., Zhai, M, Journal of Materials Chemistry 2012, 22, 5914-5916.
- 490 2 Alidokht, L., Khataee, A., Reyhanitabar, A., Oustan, S, Desalination 2011, 270, 105-110.
- 3 Lv, X., Xu, J., Jiang, G., Tang, J., Xu, X., Journal of Colloid and Interface Science 2012, 369, 460-469.
- 4 Liu, T., Wang, Z.L., Zhao, L., Yang, X., Chemical Engineering Journal 2012, 189,
495 196-202.
- 5 Arslan, G., Edeballi, S., Pehlivan, E., Desalination 2010, 255, 117-123.
- 6 Liu, B., Huang, Y., Journal of Materials Chemistry 2011, 21, 17413-17418.
- 7 Liu, X., Zhou, W., Qian, X., Shen, J., An, X., Carbohydrate Polymers 2013, 92, 659-661.
- 500 8 Liu, X., Qian, X., Shen, J., Zhou, W., An, X., Bioresource Technology 2012, 124, 516-519.
- 9 Gong, X., Li, W., Wang, K., Hu, J., Bioresource Technology 2013, 141, 145-151.
- 10 Shi, L.N., Lin, Y.M., Zhang, X., Chen, Z.L., Chemical Engineering Journal 2011, 171, 612-617.
- 505 11 Liu, T., Zhao, L., Sun, D., Tan, X., Journal of Hazardous Materials 2010, 184,

724-730.

12 Geng, B., Jin, Z., Li, T., Qi, X., *Chemosphere* 2009, 75, 825-830.

13 Geng, B., Jin, Z., Li, T., Qi, X., *Science of the Total Environment* 2009, 407, 4994-5000.

510 14 Zimmermann, A.C., Mecabô, A., Fagundes, T., Rodrigues, C.A., *Journal of Hazardous Materials* 2010, 179, 192-196.

15 Shen, C., Chen, H., Wu, S., Wen, Y., Li, L., Jiang, Z., Li, M., Liu, W., *Journal of Hazardous Materials* 2013, 244, 689-697.

16 Wajima, T., Umetsu, Y., Narita, S., Sugawara, K., *Desalination* 2009, 249, 323-330.

17 Babaeiveli, K., Khodadoust, A.P., *Journal of Colloid and Interface Science* 2013, 394, 419-427.

18 Miller, S.M., Spaulding, M.L., Zimmerman, J.B., *Water Research* 2011, 45, 5745-5754.

520 19 Jagtap, S., Thakre, D., Wanjari, S., Kamble, S., Labhsetwar, N., Rayalu, S., *Journal of Colloid and Interface Science* 2009, 332, 280-290.

20 Hasmath, F.M., Sankaran, M., *Journal of Chitin and Chitosan Science* 2013, 8, 42-49.

21 Shi, Z., Neoh, K., Kang, E., Poh, C.K., Wang, W., *Biomacromolecules* 2009, 10, 1603-1611.

22 Rajiv Gandhi, M., Kousalya, G., Viswanathan, N., Meenakshi, S., *Carbohydrate Polymers* 2011, 83, 1082-1087.

- 23 Kavitha, K., Sutha, S., Prabhu, M., Rajendran, V., Jayakumar, T., Carbohydrate Polymers 2013, 93, 731-739.
- 530 24 Al-Sagheer, F., Merchant, S., Carbohydrate Polymers 2011, 85, 356-362.
- 25 Cao, C.Y., Qu, J., Yan, W.S., Zhu, J.F., Wu, Z.Y., Song, W.G., Langmuir 2012, 28, 4573-4579.
- 26 Chen, X.G., Park, H.J., Carbohydrate Polymers 2003, 53, 355-359.
- 27 Li, X., Zhu, H., Wei, J., Wang, K., Xu, E., Li, Z., Wu, D., Applied Physics A: Materials Science & Processing 2009, 97, 341-344.
- 535 28 Abou El-Reash, Y., Otto, M., Kenawy, I., Ouf, A., International Journal of Biological Macromolecules 2011, 49, 513-522.
- 29 Park, D., Yun, Y.S., Park, J.M., Environmental Science & Technology 2004, 38, 4860-4864.
- 540 30 Lopez-Ramon, M., Stoeckli, F., Moreno-Castilla, C., Carrasco-Marin, F., Carbon 1999, 37, 1215-1221.
- 31 Sarhan, A., Ayad, D., Badawy, D., Monier, M., Reactive and Functional Polymers 2009, 69, 358-363.
- 32 Wu, Z., Li, S., Wan, J., Wang, Y., Journal of Molecular Liquids 2012, 170, 25-29.
- 545 33 Li, L., Fan, L., Sun, M., Qiu, H., Li, X., Duan, H., Luo, C., Colloids and Surfaces B: Biointerfaces 2013, 107, 76-83.
- 34 Jung, C., Heo, J., Han, J., Her, N., Lee, S.J., Oh, J., Ryu, J., Yoon, Y., Separation and Purification Technology 2013, 106(0), 63-71.
- 35 Hu, X.-j., Wang, J.-s., Liu, Y.-g., Li, X., Zeng, G.-m., Bao, Z.-l., Zeng, X.-x.,

- 550 Chen, A.-w., Long, F., Journal of Hazardous Materials 2011, 185, 306-314.
- 36 Sun, L., Zhang, L., Liang, C., Yuan, Z., Zhang, Y., Xu, W., Zhang, J., Chen, Y.,
Journal of Materials Chemistry 2011, 21, 5877-5880.
- 37 Kyzas, G. Z., Lazaridis, N. K., Kostoglou M., Journal of Colloid and Interface
Science 2013, 407, 432-441
- 555 38 Santhana K. K. A., Kumar.C.U., Rajesh, V., Rajesh,N., International Journal of
Biological Macromolecules 2014, 66, 135-143.
- 39 Xie, P., Hao, X., Mohamad, O.A., Liang, J., Wei, G. Applied Biochemistry
Biotechnology 2013, 169, 570-587.
- 40 Bulut, Y., Gözübenli, N., Aydın, H., Journal of Hazardous Materials 2007, 144,
560 300-306.
- 41 Ho, Y.-S., McKay, G., Water Research 2000, 34, 735-742.
- 42 Mohan, D., Pittman Jr, C.U., Journal of Hazardous Materials 2006, 137, 762-811.

565

570

Figure Captions

Fig. 1:

FT-IR (A) and XRD (B) spectra of the CTS (a), Ti-CTS (b), Ti-CTS-Cr (c); elemental
575 mapping images (EMI, C) of Ti-CTS and Ti-CTS-Cr; SEM images of CTS (D),
Ti-CTS (E) and Ti-CTS-Cr (F).

Fig. 2:

The wide scan XPS spectra of Ti-CTS composite without (A) and with (B) Cr(VI)
absorbed; and high resolution Cr 2p spectra of Ti-CTS-Cr composite before (C) and
580 after (D) desorption with NaOH.

Fig. 3

The effect of solution pH and concentration of Ti^{4+} leaching into solution (a); dosage
of adsorbent (b); initial Cr(VI) concentration and isotherms (c); contact time and
kinetic (d); co-existing cations and anions (e) and regeneration of Ti-CTS composite
585 (f).

Scheme 1:

The proposed adsorption coupled reduction mechanism of Cr(VI) removal by Ti-CTS
composite.

590

Tables

595 Table 1

Langmuir, Freundlich and Tempkin isotherm parameters and Pseudo-second order kinetic parameters for Cr(VI) adsorption onto Ti-CTS composite.

Adsorption isotherms parameters			Kinetic Pseudo-second-order		
Langmuir	K_L (L/mg)	0.415	parameters	Initial Cr(VI) concentration	
	q_m (mg/g)	171		30 mg L ⁻¹	50 mg L ⁻¹
	R^2	0.993		123	167
Freundlich	$\ln K_f$	4.0	q_{exp} (mg g ⁻¹)		
	n	2.54		1.53 × 10 ⁻³	4.86 × 10 ⁻⁴
	R^2	0.798		124	165
Tempkin	$\ln A$	1.35	R^2		
	B	38.8		0.9997	0.9991
	R^2	0.904		23.4	13.2

600

605

Table 2: Adsorption comparison of Ti-CTS composite and recently reported literature of adsorbents for Cr(VI).

Adsorbents	q_{\max} (mg g^{-1})	C_0 (mg L^{-1})	Time (min)	pH/ Temperature	Reference
Titanium cross-linked chitosan composite	171	10-50	420	5/25°C	Present work
Modified magnetic chitosan chelating resin	58.5	10-300	120	2/28°C	28
Cross-linked chitosan resin	86.8	20-160	120	3/25°C	32
Magnetic cyclodextrin – chitosan/grapheme oxide (CCGO)	67.66	5.0-50	300	3/30°C	33
chitosan	35.6	0.25-50	120	4/20°C	34
Ethylenediamine cross-linked magnetic chitosan resin	51.8	20-200	10	2/30°C	35
Chitosan modified Fe^0 nanowires in porous anodic alumina	113.2	10-60	400	5/30°C	36
Poly (ethylene imine) Grafted chitosan	88.4	0-50	105	4/25°C	37
n-butylacrylate grafted chitosan	17.15	0-300	60	3.5/30°C	38
Mesorbizobium amorphae Strain CCNWGS0123	47.67	10-400	1000	2/30°C	39

Table 3

The thermodynamic parameters for adsorption of Cr(VI) by Ti-CTS composite at different temperatures.

T (K)	$\ln k_d$	ΔG° (kJ/mol)	ΔH° (kJ/mol)	ΔS° (kJ/mol K)	R^2
277.15	3.016	-6.87	3.38	0.037	0.987
293.15	3.083	-7.47			
303.15	3.156	-7.84			
308.15	3.161	-8.02			

615

620

625

Table 4

630 The amount of Cr(III), Cr(VI) and total Cr in Cr(VI)-loaded Ti-CTS composite (N=3;
Desorption solution: 0.5 M NaOH; Digestion acid: HF/HCl/HClO₄ = 1.0 mL/1.0
mL/0.5 mL)

	Desorption and digestion		Direct digestion solution
	NaOH solution	Mixed acid solution	
Cr(III)	0.7%	98.7%	39.9%
Cr(VI)	99.3%	1.3%	60.1%

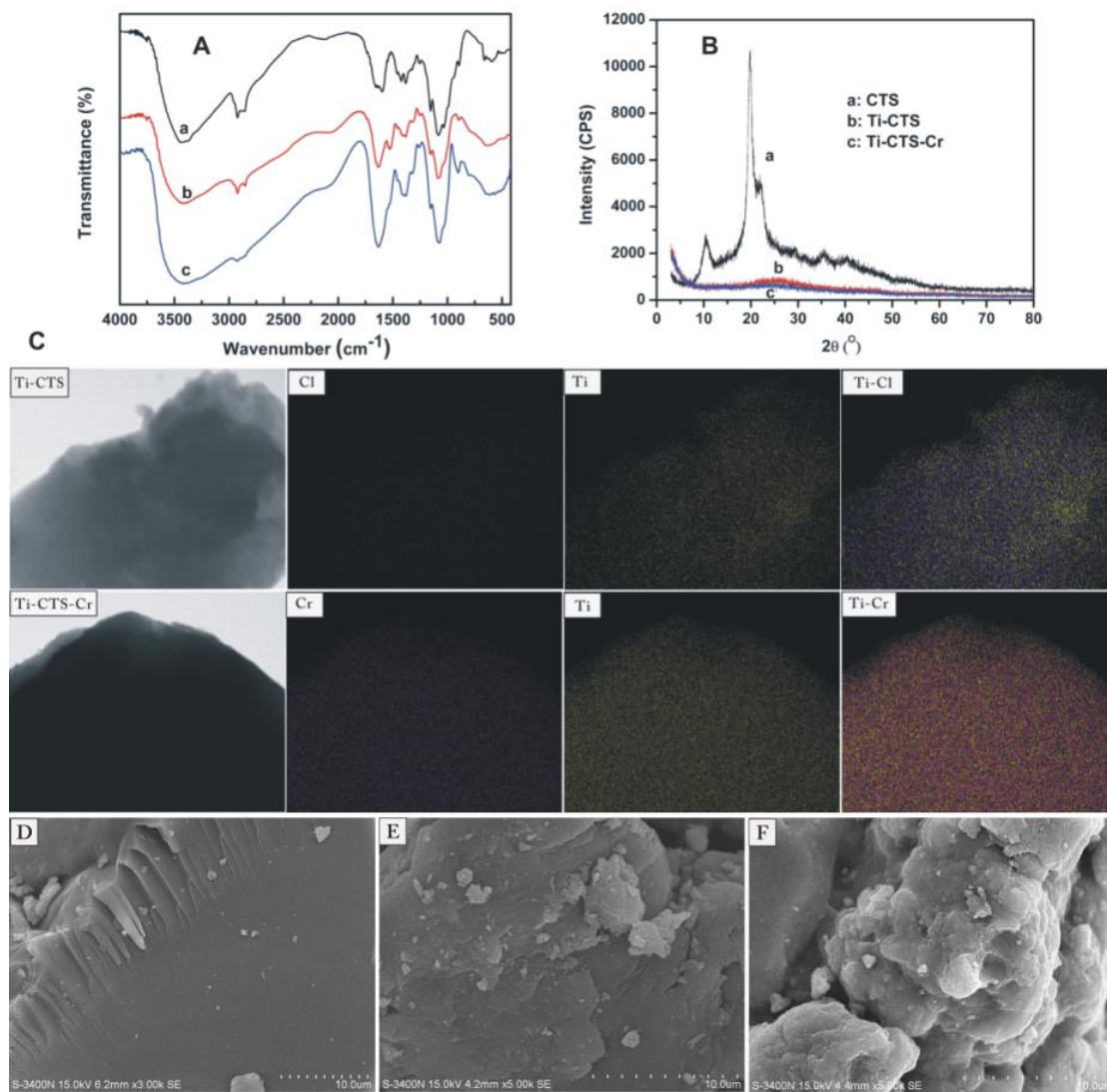
635

640

645

Figures

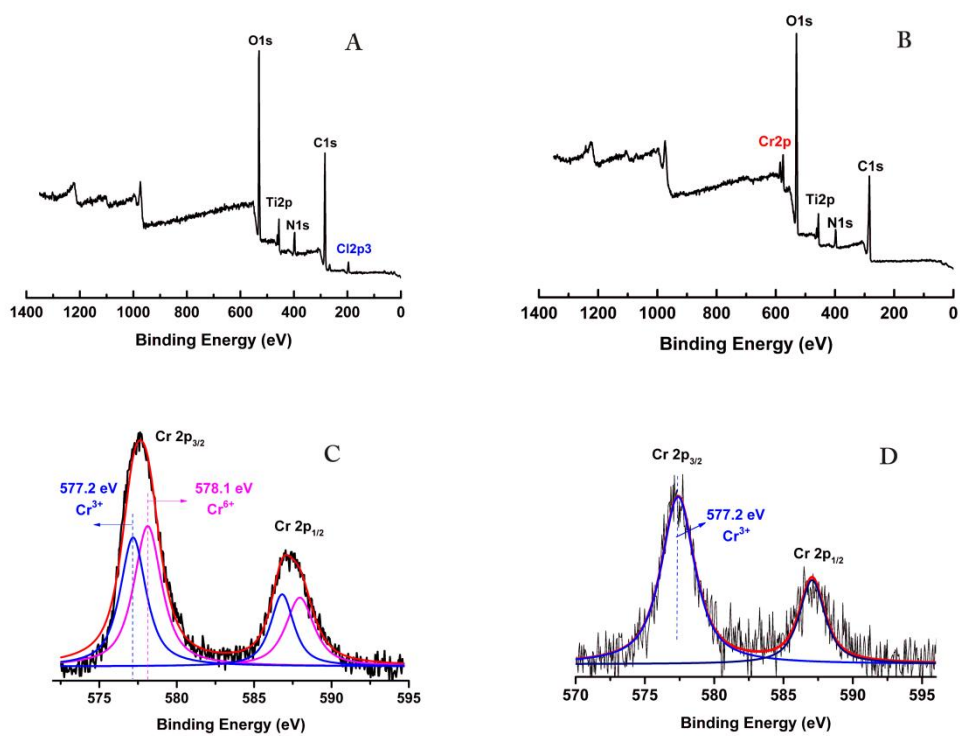
Fig. 1



650

655

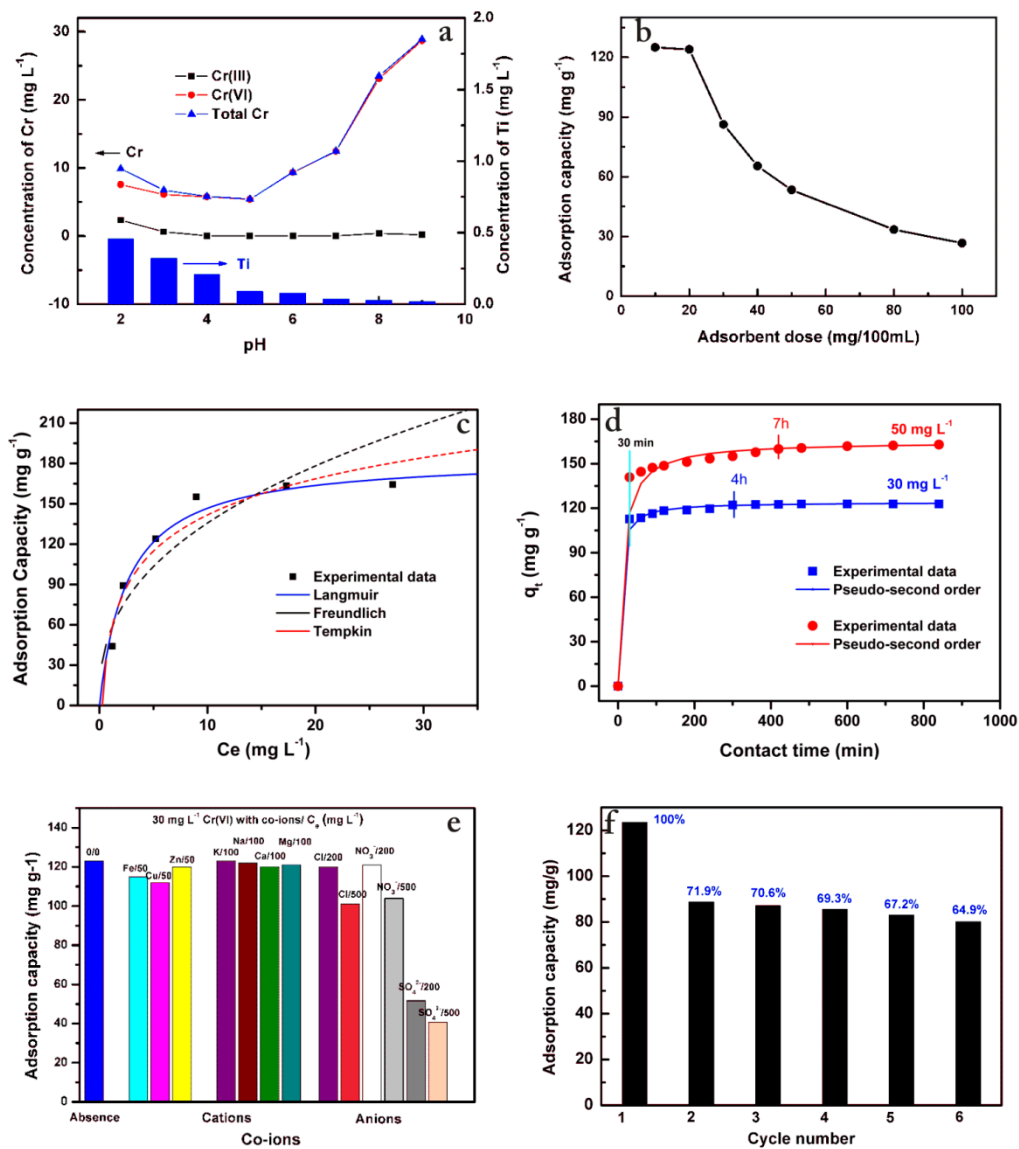
Fig. 2



660

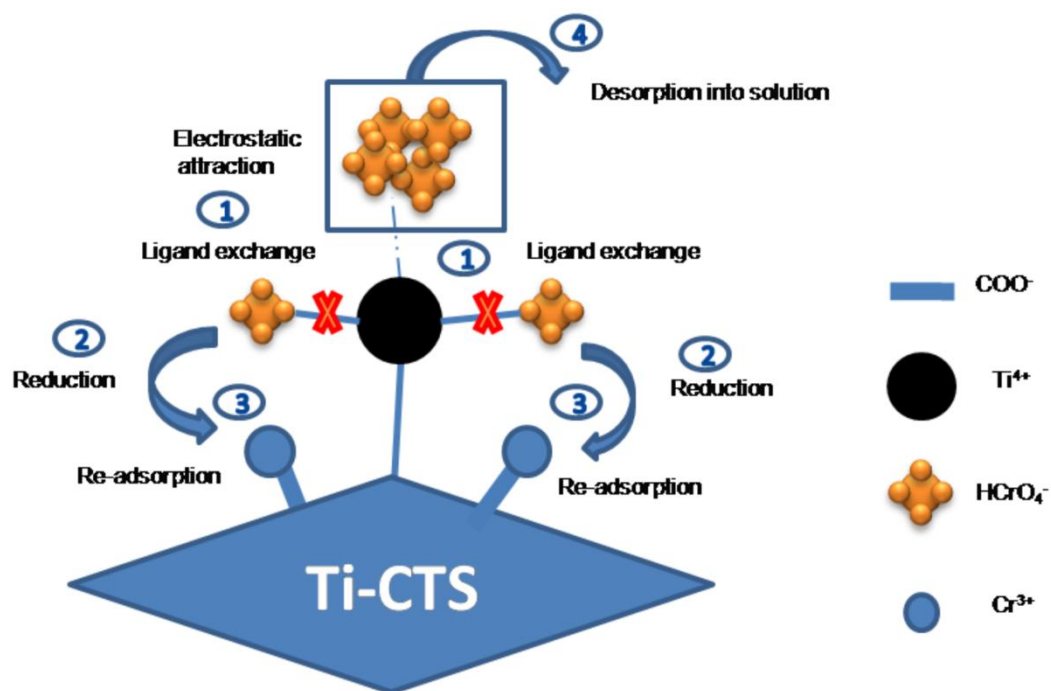
665

670 Fig.3



675

Scheme 1



680